PERSPECTIVES OF MULTI-HETEROJUNCTION HFET's FOR POWER AMPLIFICATION IN MILLIMETER WAVE RANGE

Y. Crosnier, D. Théron, B. Bonte, T. Coupez

DHS - IEMN - UM CNRS 9929
Université des Sciences et Techniques de Lille
59655 VILLENEUVE D'ASCQ CEDEX - FRANCE

ABSTRACT

There is a considerable interest in the development of high power, high efficiency HFETs for millimeter wave applications. Thanks to the great progress accomplished during the last few years in MBE growth multiheterojunction devices have reach such a maturity that they now offer attractive capabilities. This paper reports on results obtained with especially designed structures and discusses their optimization on the basis of modelling and characterizations. It shows that devices with more than 1A of drain current, 10 V of Breakdown voltage, 60 GHz of cut-off frequency ar now within the realm of possibility.

Keywords : multiheterojunction structures, millimeter power HFET.

1. INTRODUCTION

Pseudomorphic InGaAs HFET's have demonstrated their ability to operate at frequency as high as 35 GHz with almost 1 watt per mm gate width output power, 45 % power added efficiency and 6 dB gain (Ref. 1). As a proof of this maturity amplifier systems fully based on this technology are emerging (Ref. 2). The question that now arises is wether further improvements could be provided and by what means. An answer to this question is given by multi-heterojunction devices, that is the devices having more than two active heterojunctions (DH HFET) and exhibiting a multichannel structure. Various works have been done (Ref. 3, 4) in the area. The present paper provides our own experience in this field using the AlGaAs-GaAs system but also a hybrid AlGaAs-GaAs-InGaAs system.

2. MULTICHANNEL HFET BASIC PRINCIPLE

The basic structure configuration that has been chosen is depicted in figure 1. It exhibits 2 quantum wells and 3 heterojunctions supplied by 2 doped planes δ_1 and δ_2. This appears as a good trade-off for :

- a high drain current together with a reasonable Breakdown voltage.

- the possibility to get transconductance and current gain cut-off frequency profiles nearly flat, versus the gate-source voltage, by an adequate choice of the planar doping densities $N\delta_1$ and $N\delta_2$ and of the layers thicknesses. In such a structure the roles played by the middle AlGaAs layer separating the two GaAs quantum wells and by the charge density $N\delta_2$ of the bottom doped plane are predominant. The analysis of their influence and optimization have been performed on the basis of a self-consistent 1D Schrödinger-Poisson model of the charge control. In this one the doped planes are represented by thin uniformly doped layers

and the percentage of ionized dopants is established according to the Fermi statistics with the simplifying assumption of a average donor level at an arbitrary energy E_d below the conductor band. Typical results of simulation are shown in figure 2. They correspond to two variants (a) and (b) of multichannel structures with a strong coupling and where the only variable is the bottom planar doping charge $N\delta_2$. For comparison case (c) is an illustration of a classical DH structure where the thickness of the bottom AlGaAs layer is large enough to confine electrons in the single GaAs quantum well. The curves presented in these figures deal with the electron gas density N_S, the free electron density N_{AlGaAs} in AlGaAs, and their derivatives versus the gate-source voltage but under quasi-state conditions. The situation is necessarily different under microwave conditions because of the time constant associated with the donor states. As a consequence the non-linearity will be less pronounced in microwave conditions than in quasi-static ones.

3. AlGaAs-GaAs REALIZATIONS

Numerous devices have been processed according to the above design rules with varying the amount of the charges $N\delta_1$ and $N\delta_2$. Two examples are given in figures 3 and 4. Figure 3 deals with a device having $N\delta_1 = 4\ 10^{12}$ cm^{-2} $N\delta_2 = 2.5\ 10^{12}$ cm^{-2} and a T gate of about 0.3 µm in a 1.5 µm source to drain spacing (CHS 470). Its maximum drain current is 700 mA/mm. The quasi-static transconductance exhibits clearly two peaks as expected from theory and attains 300 mS/mm. A similar behaviour is obtained for the intrinsic microwave transconductance (extracted from S parameters) with a maximum lying around 400 mS/mm. The corresponding gate-source capacitance profile is weakly varying over the totality of the gate-source voltage swing. As a consequence the intrinsic current gain cut-off frequency f_c has also a remarkably flat profile comprised between 50 and 60 GHz for the whole gate voltage swing.

Figure 4 shows results for a structure where $N\delta_1$ and $N\delta_2$ are $2.5\ 10^{12}$ and $1.5\ 10^{12}$ cm^{-2} respectively, the gate length being of 0.4 µm. Such a structure has been used to realize devices with a large gate development by means of air bridges and tree configurations (CHS 432). As shown in the accompagnying table the increase of the gate width from 2x100 µm to 8x100 µm decreases somewhat the performances but these ones remain very interesting : a MAG of 7 dB at 15 GHz with 550 mS/mm of intrinsic transconductance for the 800 µm device. Moreover these two quantities present a remarkable flatness over the full range of the gate voltage swing.

4. HYBRID AlGaAs-GaAs-InGaAs REALIZATIONS

The basic idea of this other structure is to improve the gate charge control and consequently the transconductance near the pinch-off with replacing the bottom GaAs quantum well by an InGaAs one. Such an arrangement is expected to substantially increase the magnitude of the second transconductance peak (near pinch-off) owing to the higher confinement provided by InGaAs material. Figure 5 shows the structure which was investigated and its results. Two similar epilayers of this type were grown simultaneously at Thomson LCR and our Laboratory, with $N\delta_1$ and $N\delta_2$ planar doping densities of about $3\ 10^{12}$ and $4\ 10^{12}$ cm^{-2}. They were processed (CHS 471 and 496) using the same pattern with a 0.3 µm T gate. Similar performances were obtained for the two device series : a drain

current of 800-1000 mA/mm, quasi-static and microwave transconductances of about 500 and 600 mS/mm respectively, and an intrinsic current gain cut-off frequency reaching almost 70 GHz. These superior results and the unique flatness of the transconductance profile let's envisage a remarkable linearity and large current swing capabilities.

5. BREAKDOWN OPTIMIZATION

The excellent current drive and frequency response capabilities of multichannel HFET's are not sufficient to ensure high power performance. The Breakdown voltage needs also to be optimized. We are pursuing a wide study on this question both theoretically and experimentally. The present status of our investigations is as follows :

- the theoretical analysis of the potential distribution close to pinch-off within the structure indicates a strong two dimensional behaviour in the gate to drain region resulting in a very high peak electric field E_{max} at the gate edge ;

- E_{max} is strongly dependent on the total planar doping charge $N\delta_1 + N\delta_2$, the thickness "a" of the NID AlGaAs layer under the gate and the gate to drain recess spacing "d". Under the worse conditions, that is with $N\delta_1 + N\delta_2 > 5\ 10^{12}$ cm-2, a < 200 Å and d < 300 Å, Emax may reach $2\text{-}3\ 10^6$ V/cm.

- From this theoretical approach, Breakdown should mainly occur from Tunneling rather than from impact ionization. As shown in figure 6, calculations based on this assumption give reasonable but somewhat pessimistic predictions which indicates that the reality is somewhat more complex.

- Experimentation globally corroborates the theoretical analysis. As a typical illustration of the reverse gate current characteristics, figure 7 shows measurements corresponding to a device described in part 4 (CHS 471). Breakdown voltages of about 7-8 volt are possible even in the case of high planar doping levels ($N\delta_1 + N\delta_2 = 7\ 10^{12}\ cm^{-3}$). As a general rule measurements performed at various temperatures indicate, as shown in figure 7, a null or positive variation of the gate current which confirms that Breakdown results probably from a mixing of Tunneling and Impact ionization. An other important point elucidated by experiment, and shown in figure 8, is the dependence on the gate to drain spacing. Measurements carried out on devices of Thomson LCR having an asymmetrical recess spacing have demonstrated a Breakdown voltage increase of about 4 V when the recess spacing is increased from 500 nm to 3 500 nm.

6. CONCLUSION

The above results prove the superior interest of triple heterojunction double quantum well HFET's for power applications. Measurements of power performances of these devices in the 26-40 GHz band are underway and will be next supplied.

ACKNOWLEDGEMENTS

This work has been carried out with the financial help of the ESPRIT project 5032 AIMS. We are grateful to Dr. D. Pons and his research group of Thomson LCR for helpful cooperation

7. REFERENCES

1. Lester L.F., et al. 1989, DRC.
2. Smith P.M., et al. Jan. 1991, Electr. Lett. Vol. 27, n° 3.
3. Saunier P., et al. Sept. 1986, IEEE, Vol. EDL 7, n° 9.
4. Daembkes H., Weimann G., April 1988, Appl. Phys. Lett., 52 (17).

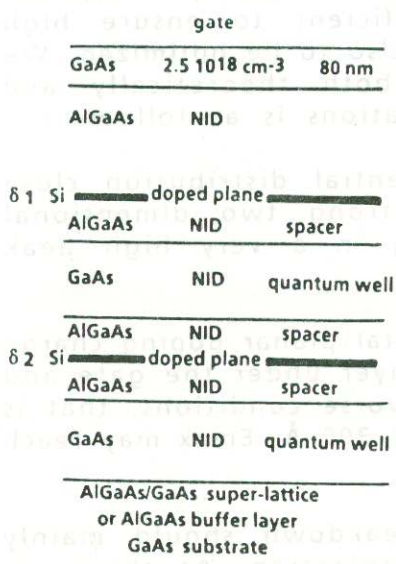

Figure 1 : The basic multichannel HFET structure under investigation.

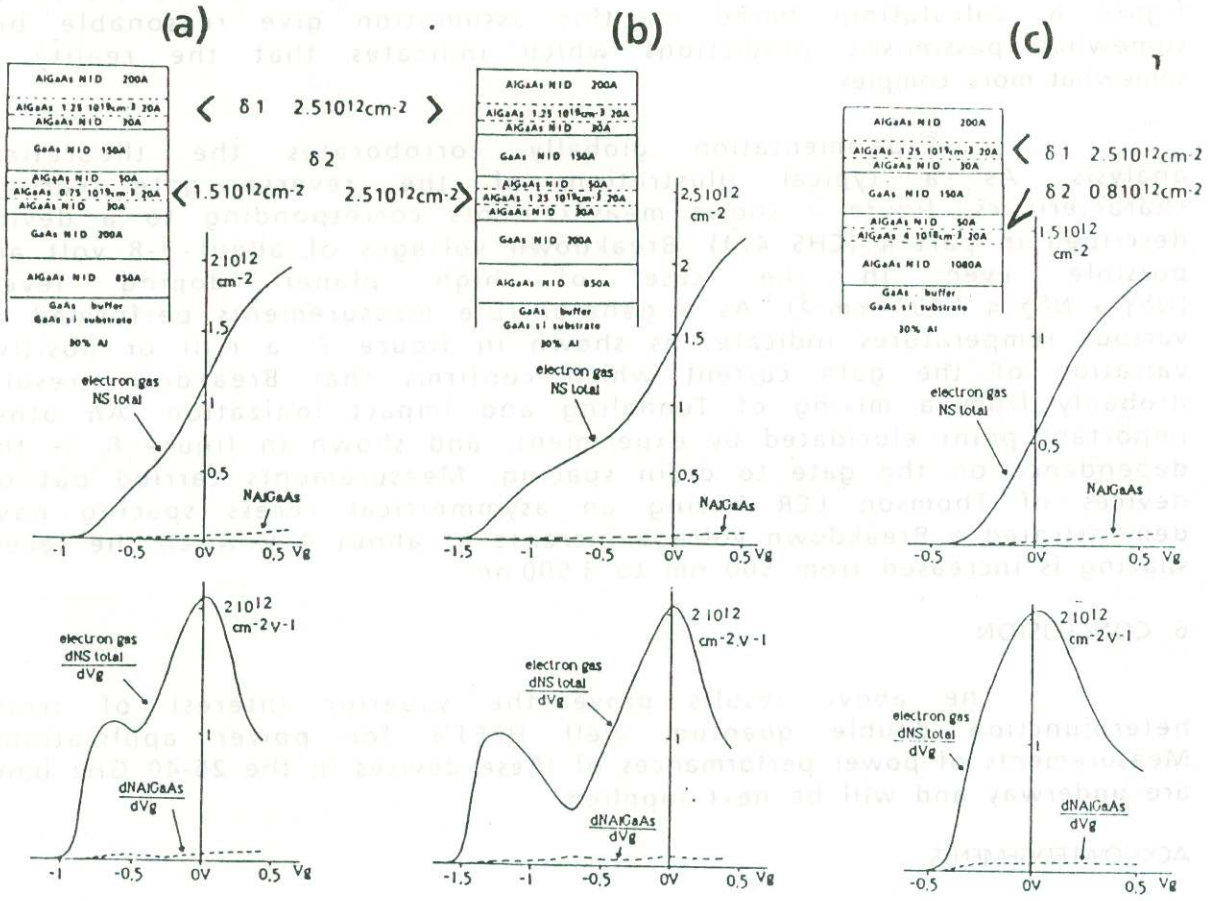

Figure 2 : Typical examples of charge control simulations corresponding to a multichannel HFET(a), (b) and for comparison, to a single channel HFET (c).

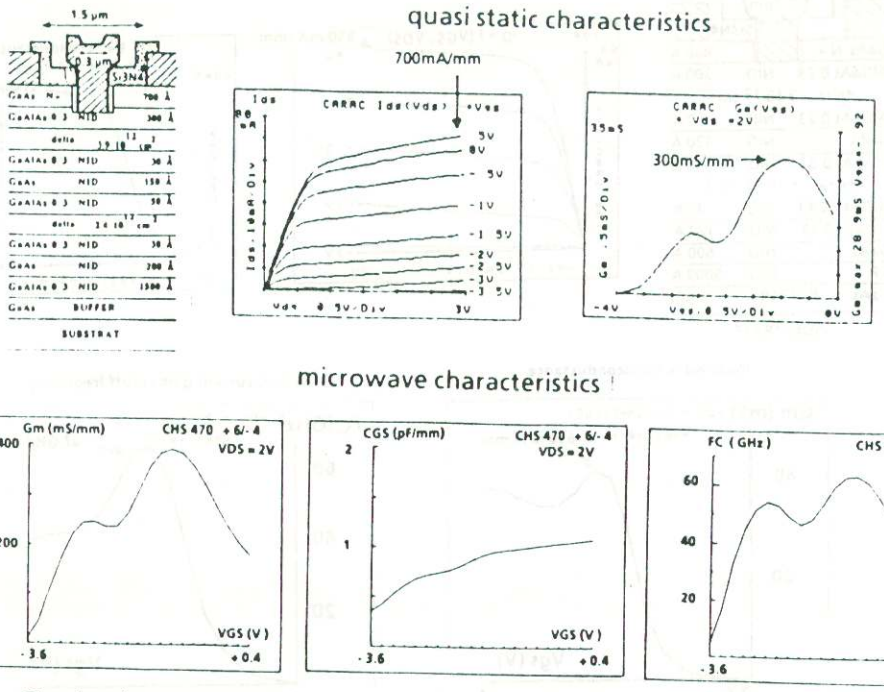

Figure 3 : Typical example of DC and microwave characteristics of a multichannel AlGaAs-GaAs HFET (CHS 470).

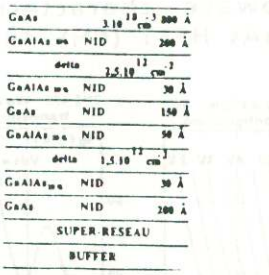

Topologie du transistor	I_{DSS}	G_m ext	G_m int	MAG à 15 GHz	h_{21} à 15 GHz	f_c max
2x100 µm (A)	100 mA (500 mA/mm)	81 mS (405 mS/mm)	97 mS (485 mS/mm)	10 dB	6.1 dB	48 GHz
8x100 µm (B)	320 mA (400 mA/mm)	314 mS (392 mS/mm)	460 mS (575 mS/mm)	6.5 dB	6.4 dB	38 GHz
8x100 µm (C)	360 mA (450 mA/mm)	311 mS (388 mS/mm)	440 mS (550 mS/mm)	7 dB	9.22 dB	36 GHz

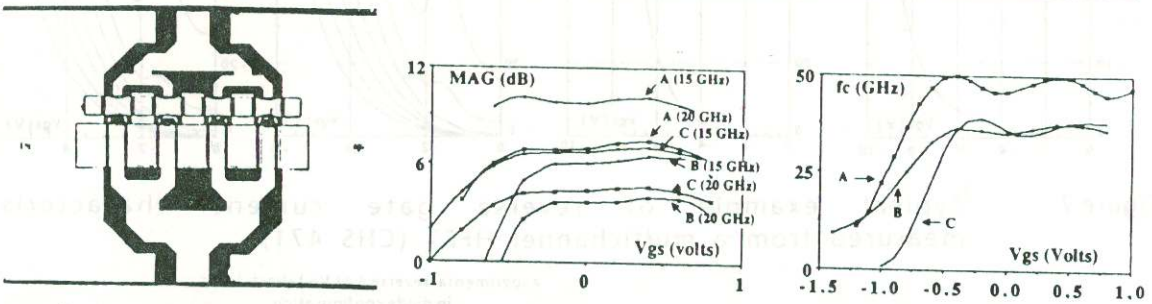

Figure 4 : Example of a power multichannel HFET based on a tree configuration (CHS 432).

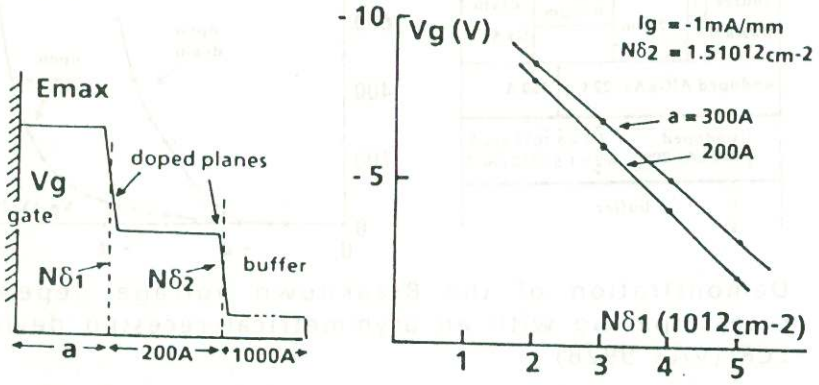

Figure 6 : Theoretical variation of the Breakdown voltage versus the planar doping density corresponding to a Tunnel current density of 1 mA/mm.

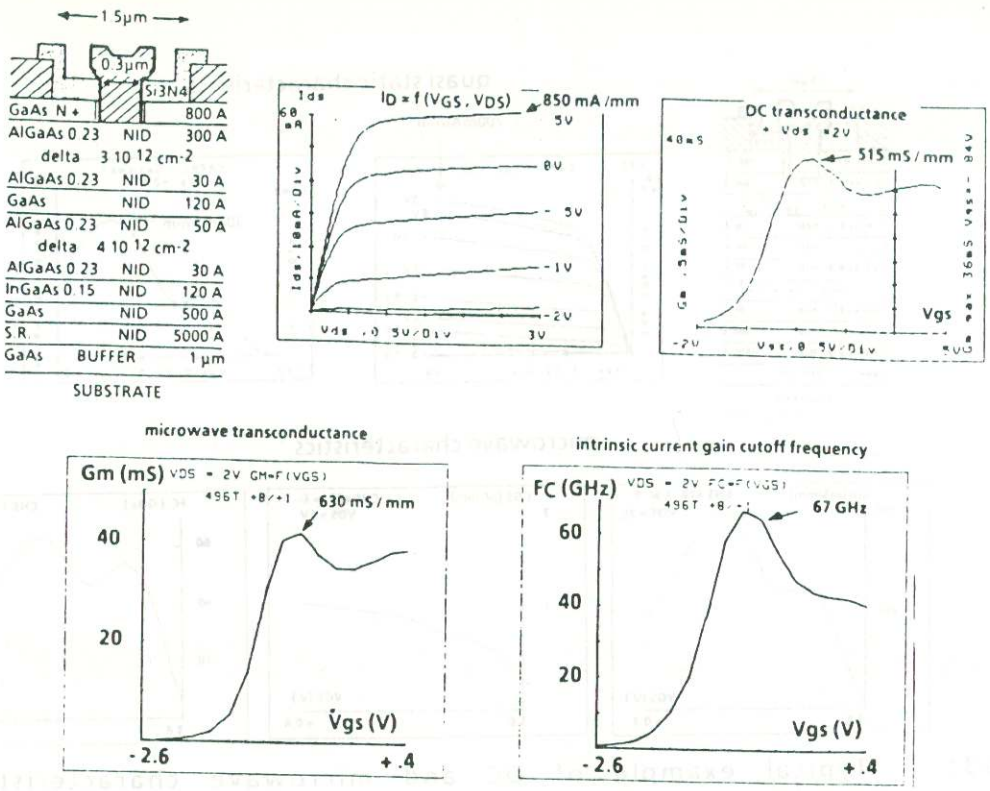

Figure 5 : Typical example of DC and microwave characteristics of a hybrid multichannel AlGaAs-GaAs-InGaAs HFET (CHS 496).

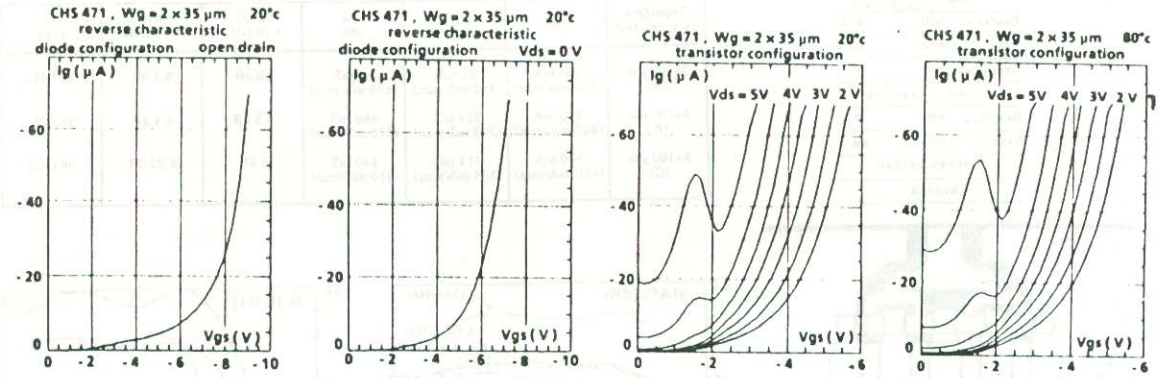

Figure 7 : Typical example of reverse gate current characteristics measured from a multichannel HFET (CHS 471).

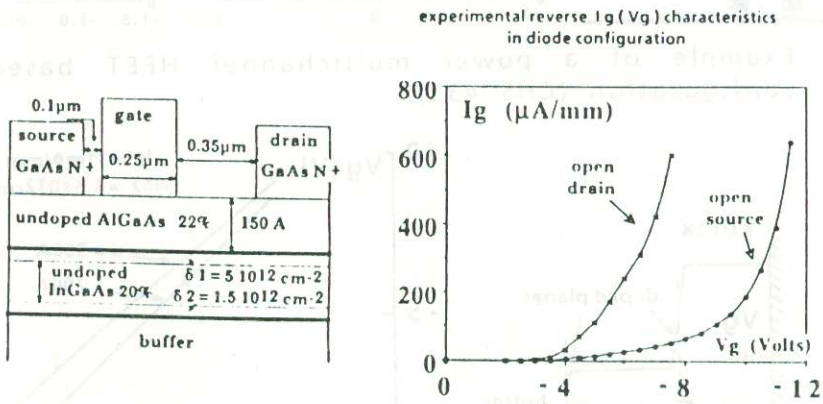

Figure 8 : Demonstration of the Breakdown voltage dependence on the recess spacing with an asymmetrical recessed device of Thomson LCR (VAR 992B).